

Microangiopathy in temporal lobe epilepsy with diffusion MRI alterations and cognitive decline

Joan Liu

UCL Queen Square Institute of Neurology

Lawrence Binding

University College London

Isha Puntambekar

UCL Queen Square Institute of Neurology

Smriti Patodia

UCL Queen Square Institute of Neurology

Yau Lim

UCL Queen Square Institute of Neurology

Alicja Mrzyglod

UCL Queen Square Institute of Neurology

Fenglai Xiao

UCL Queen Square Institute of Neurology

Shengning Pan

University College London

Remika Mito

University of Melbourne

Jane deTisi

UCL Queen Square Institute of Neurology

John S Duncan

UCL Queen Square Institute of Neurology

Sallie Baxendale

UCL Queen Square Institute of Neurology

Matthias Koepp

UCL Queen Square Institute of Neurology

Maria Thom

m.thom@ucl.ac.uk



UCL Queen Square Institute of Neurology

Research Article

Keywords: White matter, Temporal lobe epilepsy, microangiopathy, Diffusion MRI, Fixel based analysis, cognitive decline

Posted Date: September 4th, 2024

DOI: <https://doi.org/10.21203/rs.3.rs-4841682/v1>

License:   This work is licensed under a Creative Commons Attribution 4.0 International License. [Read Full License](#)

Additional Declarations: No competing interests reported.

Abstract

White matter microvascular alterations in temporal lobe epilepsy (TLE) can influence local hemodynamics and are relevant to understanding acquired neurodegenerative processes and cognitive impairment associated with this condition. We quantified microvascular changes, myelin, axonal and glial/matrix labelling in the gyral core and deep temporal lobe white matter regions in surgical resections from 44 TLE patients with or without hippocampal sclerosis. We compared this pathology data with in-vivo MRI diffusion measurements in co-registered regions and neuropsychological measures of pre-operative cognitive impairment and decline. We observed increased arteriolosclerosis in TLE compared to controls (greater sclerotic index, $p < 0.001$) which was independent of age. Microvascular changes included increased vascular densities in some regions but uniformly reduced mean vascular size (COL4, $p < 0.05$ to 0.0001), and increased pericyte coverage of small vessels and capillaries particularly in deep white matter (PDGFR β and SMA, $p < 0.01$) which was more marked the longer the epilepsy ($p < 0.05$). We noted increased glial numbers (Olig2, Iba1) but reduced myelin (MAG, PLP) in TLE compared to controls, particularly prominent in deep white matter. Gene expression analysis showed a greater reduction of myelination genes in HS than non-HS cases and with age and correlated with diffusion MRI alterations. Glial densities and vascular size were increased with increased MRI diffusivity and vascular density with Fixel-Based analysis white matter regions. Increased perivascular space associated with reduced fractional anisotropy as well as age-accelerated cognitive decline prior to surgery ($p < 0.05$). In summary, likely acquired microangiopathic changes in TLE, including vascular sclerosis, increased pericyte coverage and reduced small vessel size, may indicate a functional alteration in contractility of small vessels and haemodynamics that could impact on tissue perfusion. These morphological features are detectable in-vivo on white matter diffusion MRI and might explain cognitive decline in TLE.

Introduction

There is a growing body of evidence that microvascular dysfunction occurs in epilepsy which is detrimental to both seizure control and its comorbidities [47, 51]. Degenerative small vessel disease of the white matter contributes to leading causes of dementia including subcortical vascular dementia [43] and Alzheimer's disease [30]. Pathological alterations of the white matter in epilepsy, including temporal lobe epilepsy (TLE), have recognised small vessel disease (SVD), abnormal vascular collagen deposition, angiogenesis and altered pericytes while other studies have demonstrated degeneration of white matter axons and myelination [2, 9, 12, 19, 20, 25]. One hypothesis proposes that microvascular pathology in epilepsy impacts on white matter haemodynamics, blood brain barrier (BBB) function and myelin integrity [64] but this has yet to be fully confirmed in surgical tissue samples. Experimentally, ictal contractions of pericytes have been shown to induce vasospasm and ischaemia-related neurodegeneration [34] and pericyte injury in epilepsy leads to neurovascular decoupling [47] with a dynamic reorganisation proportional to seizure severity [3]. BBB dysfunction in experimental seizures [39], has also been demonstrated following a single seizure in patients [57] and recently associated with cognitive impairment in TLE [52]. Furthermore, SVD is itself associated with late onset seizures [15], with proposed mechanisms for epileptogenesis including impaired cerebral perfusion and disruption of subcortical networks [73].

It has long been established that memory impairment and cognitive dysfunction are key features and a significant co-morbidity of TLE with a wide variability in outcome following surgical treatment [6]. Studies have

largely focused on neuronal loss driven acquired hippocampal pathology [35, 66, 76] but this does not fully explain the clinical picture and the contribution of vascular dysfunction is under-investigated [52]. Diffusion weighted MRI (DWI) of white matter in epilepsy show widespread reduction of fractional anisotropy (FA) and increased mean diffusivity (MD) in TLE (Hatton 2020) and studies have identified changes specifically in the subcortical white matter [36, 68] and shown a link with cognitive phenotypes, memory and language impairment [53]. Fixel-based diffusion analysis (FBA) has an additional potential to decipher microstructure alterations in the complex fibre organization of superficial white matter [13].

In a cohort of TLE patients with well-characterized pre-operative neurocognitive function, our aim was to explore regional differences of white matter pathology in superficial versus deep white matter, particularly for evidence of a microangiopathy, and compare with MRI diffusion measures (DWI and FBA).

Methods and Materials

Case selection

Cases were obtained from the Epilepsy Society Brain and Tissue Bank (ESBTB) at University College London Queen Square Institute of Neurology. We included 44 adult patients who had undergone an anterior temporal lobe resection for the treatment of drug-refractory TLE with a pathological and MRI diagnosis of either hippocampal sclerosis (HS, n=33, left n=21) or non-lesional without HS (non-HS, n=11, left n=6). For 24 of those 44 patients, DWI data as available. Tumours, cortical dysplasia, cavernomas or other focal lesions were excluded but some cases showed patchy cortical neuronal loss and gliosis but without a specific diagnosis. All individuals having epilepsy surgery consented for use of tissue and linked clinical data in research. Control cases (post-mortem samples) were selected from the ESBTB and the MRC Edinburgh Brain and Tissue Bank (EBTB) who were non-epilepsy controls (NEC; n= 28) with no neurological disease or neuropathology following brain examination and epilepsy controls (EC; n=28) with no lesional brain pathology at post-mortem, no history of temporal lobe epilepsy who had died from sudden and unexpected death in epilepsy (SUDEP). Case details are summarised in Table 1 with further details in supplemental Table 1 including any cerebrovascular disease risk factors and detail of cause of death. For gene expression studies a cohort of 36 cases was selected including TLE with HS (n=16) and non-lesional TLE (n=6), non-lesional frontal-lobe epilepsy (n=6), non-lesional post-mortem EPC (from ESBTB, n=4) and NEC (from EBTB, n=4). The 22 TLE cases represented a range of ages at surgery (10 <40 years at surgery; 12 > 40 years at surgery). We excluded cases with prior stereoencephalography (SEEG) investigations to avoid inclusion of electrode track scars in white matter (Table 1).

Tissue preparation for pathology measures

A tissue block representing a coronal section through the superior (STG), middle (MTG), inferior (ITG) and fusiform temporal gyrus (FG) was selected from surgical cases at 1.5 cm from the temporal pole. The temporal gyri had been marked following surgery for gyral orientation and correlation with the pre- and post-operative MRI was also used for further anatomical alignment in some cases. The tissue was formalin-fixed, routinely processed, and serial sections cut at 5-micron intervals. For control cases, formalin-fixed paraffin-embedded tissue blocks from both hemispheres, from STG and MTG were used where available, and similarly sectioned.

This resulted in a final group of 104 temporal lobe samples for investigation, although not all gyral regions were available in all cases and controls (see supplemental Table 1 for regions available in each case).

Vascular sclerosis measurements: We used the sclerotic index (SI), a standard method used in vascular dementia to quantify degenerative small vessel pathology on H&E sections (Supplemental Figure 1A and methods).

Immunostaining analysis and quantitation

A panel of antibodies for white matter structures and vessels was used and standard immunohistochemistry was carried out. The rationale for selection is summarized in Table 2 and staining protocols further detailed in the supplemental methods. Double-labelling immunofluorescence for PDGFRb and smooth muscle actin (SMA) was carried out on 4 TLE cases and 4 controls (Supplemental Table 1 and methods). Slides were scanned with a NanoZoomer S360 Digital slide scanner (C13220-01) at 40x magnification as a single z-stack and immunofluorescence sections with a Hamamatsu NanoZoomer S60 Digital slide scanner (C13210-04, Hamamatsu Photonics K.K). Using QuPath software (Version 0.4.1, [4]) white matter regions of Interests (ROIs) were defined from each available gyrus, further divided into 'core' and 'deep' white matter using an anatomical boundary of straight line joining the bottom of two adjacent gyri (Supplemental Figure 2). The core white matter therefore represented the superficial and subcortical 'U' fibres but excluding cortical grey matter; any tissue artefacts were also excluded. Using QuPath intensity thresholds were set at three levels for each marker (low, medium and high thresholds) and optimal thresholds selected to maximize specific and minimizing non-specific detection (see supplemental Figure 3), keeping thresholds constant across all cases and controls. A labelling index was calculated for each ROI (i.e. a field fraction of total labelled area). In addition, cell density measurements on NeuN and Olig2 sections were determined using Qupath Cellpose extension (<https://github.com/BIOP/qupath-extension-cellpose>) [46, 63] (Supplemental Figure 3, Supplemental methods).

PDGFRb analysis, vascular structures and glia:PDGFRb highlighted pericytes and perivascular cells in addition to small multipolar parenchymal cells not associated with vessels. PDGFRb was therefore manually quantified for vascular structures in addition to automated labelling index (See Supplemental methods). PDGFRb+ vascular structures of all size were classified into Type 1 or Type 2 vessels, according to either complete or partial vascular PDGFRb+ pericyte coverage respectively (Supplemental Figure 1B) and also categorized as capillary (<5 microns), capillaries (5 to £10 microns), small arterioles (10 to £25 microns) and arterioles (>25 microns) and the density and proportion of vessel types in each ROI calculated.

COL4 and SMA vascular structures:To evaluate the density of white matter COL4+ vessels and diameters, an automated method was developed in Qupath (YML) and vessel density/mm² and median vascular diameter for each ROI calculated (Supplemental Figure 1C-G). A similar but modified approach was carried out for SMA but, as perivascular cell labelling was often discontinuous, SMA vessels were also categorized as Type 1 if the labelling was circumferential or Type 2 if discontinuous (Supplemental Figure 4 and methods). For PDGFRb/SMA double labelling, 2mm² ROI were quantified using NDP.view2 software in STG and MTG core and deep white matter for the density of double and single labelled vessels and vessel diameters, distinguishing type 1 or 2 SMA+ vessels.

White Matter gene expression data

Total RNA was isolated from the deep white matter of 36 cases (the gyral core regions were not separately analysed) and processed for Nanostring nCounter analysis using NanoString Neuropathology Gene Expression panel (XT Hs NeuroPath CSO; NanoString Technologies, Washington, USA), which target genes involved in neuroplasticity, development and aging, neuroinflammation, metabolism and maintenance of structural integrity pathways (Supplemental methods). Visualisation of data through constructions of heatmaps, correlative matrices and graphs were achieved using nSolver software (version 4.0, NanoString, Washington, USA). Multivariate linear modelling was performed to identify significant differentially expressed genes in different comparative groups divided as follows: Pathology (HS/Non-lesional), age of Surgery (under/over 40 years), TLE (surgical/PM controls).

Diffusion MRI analysis

The study included 24 patients with pre-operative DWI, including 10 with gene expression data (Supplemental Table 1), and was compared to 70 healthy controls. Methods are provided in detail in supplemental files. In brief, structural 3D T1-weighted (MPRAGE; 1mm isotropic resolution) MRI images were aligned with pathology resection. Using Freesurfer (version 7, [18]) the white matter was parcellated into superficial and deep STG, MTG and ITG regions. The image was then rotated back to the diffusion image to extract tensors, including the mean diffusivity (MD) and fractional anisotropy (FA) axial diffusivity (AD), radial diffusivity (RD).

Fixel-based analysis (FBA) : An FBA framework was applied [49]; 'fixel' refers to a specific fibre population within a single image voxel, computed based on segmentation of the computed WM orientation distribution functions (ODFs) with correspondence established between subject-specific fixels and those of the WM ODF template [49]. We utilised fibre density and cross-section metric which was obtained at each white matter fixel. This metric combines microstructural and morphological information, such that it is sensitive to changes in the density of fibres passing in a particular direction within a given voxel, as well as the changes in the cross-section of fibre bundles that traverse multiple image voxels. Connectivity-based smoothing was performed on fixel-based measures for all participants [48].

Clinical data and neuropsychometry

Clinical data regarding age of onset and duration of seizures was retrieved from case records. Patients underwent a comprehensive set of standard neuropsychometric tests pre-operatively. This battery has been described previously [5] and further detailed in supplemental methods. Data were available for 43 patients and patients were binarized into "decline" or "stable" groups based on their pre-surgical verbal cognitive abilities. A discrepancy of 10 or more between the estimated pre-morbid intelligence and VIQ/VCI was considered clinically relevant cognitive decline [44].

Statistical analysis

Statistical analysis was conducted using SPSS (IBM corporation, Version 29) and Graph Pad Prism software (Supplemental methods). Non-parametric tests were used for comparison of pathology variables between groups and Wilcoxon signed rank test for differences between superficial and deep white matter. For RNA analysis, Benjamini-Hochberg adjusted p values were presented as shown, otherwise unadjusted p values were

noted ; $p < 0.05$ was considered statistically significant. Pathway analyses were performed based on Gene Set analysis score, taking to account t-statistics and plots were generated from pathways scores to show variations between groups. Logistic regression analysis was used for comparison of pathology variables between neuropsychology groups using SPSS for multiple imputation of any missing pathology variables. Univariate linear regression analysis was conducted for comparison between DWI and pathology Z scores, with significance taken at $p < 0.05$.

Results

Comparisons between epilepsy and control groups

White matter myelination and glia

On qualitative analysis of TLE cases, MAG showed more intense labelling of myelinated axons in the gyral core and cortical radial fibres than the deep white matter (Fig. 1A-C) whereas more uniform labelling was noted in control PM white matter (Fig. 1D). PLP findings were similar to MAG but with an overall reduced intensity (Fig. 1F-I). Relatively uniform patterns of axonal labelling were noted in both core and deep white matter in TLE with neurofilament markers (NF-L, NF-M and NF-L) (Supplemental Fig. 5C-E). Olig2 showed diffuse increase in white matter oligodendroglia in TLE (Fig. 1K-N) and Iba1, increased white matter microglia relative to cortex and controls (Fig. 1P-S). PDGFR β highlighted pericytes in relation to vessels in addition to scattered single multipolar-glia cells through the white matter and cortex (Fig. 1U-W). In TLE cases there was a clear gradient, with increased numbers in deep compared to gyral core white matter and qualitatively fewer PDGFR β -positive glial cells in controls (Fig. 1X). NeuN labelled single interstitial neurons in both core and deep white matter in TLE and control groups (Supplemental Fig. 5A). Tenascin C showed predominant expression in the white matter matrix, extending into the deep cortex in some areas around blood vessels and glial cells (Supplemental Fig. 5B).

Quantitation of MAG was significantly lower in TLE than NEC and EPC in STG and MTG core and deep white matter ROIs ($p < 0.001$ and $p < 0.05$); PLP was significantly lower in TLE than NEC in these regions ($p < 0.05$) but not EPC (Fig. 1E,J, Suppl Table 2). In contrast, Olig2 density, PDGFR β and Iba1 LI, were all significantly higher in white matter ROI in TLE than controls ($p < 0.001$) but with greater differences noted between TLE and NEC than EPC groups (Fig. 1O,T,Y, Suppl Table 2).

White matter microangiopathy

In some TLE cases scattered medium sized white matter vessels showed variable degrees of hyaline thickening of the vessel wall (vascular sclerosis/SVD) on H&E (Fig. 2A) although this was not evident in all vessels or cases. PVS expansion, with pigment laden macrophages and corpora amylacea was noted around some vessels, including those without sclerosis (Fig. 2B-D). COL4 + highlighted the basal lamina of white matter vessels of all calibre (Supplemental Fig. 1C). Frequent findings were 'splitting' of the COL4 + layer to produce a double-layer, particularly in vessels with expanded perivascular spaces and sclerosis (Fig. 2E-G). This microvascular dissection was not appreciated with PDGFR β or SMA (Fig. 2H). PDGFR β (Fig. 2I,K) and SMA (Fig. 2H,J) labelling was noted in arterioles and also the smallest capillaries. Vessels showed continuous circumferential labelling with SMA or PDGFR β (termed Type 1) or discontinuous labelling (Type 2) in both TLE

and controls (Fig. 2I,K and Supplemental Fig. 4D,E). Double labelling with PDGFR β /SMA in selected cases and controls confirmed co-localisation of labelling in some arterioles and capillaries (Fig. 2R-U), however many smaller capillaries were PDGFR β + /SMA- (Fig. 2U), whereas PDGFR β - /SMA + vessels were not observed in either TLE or controls.

Vascular sclerotic index

In cerebrovascular disease an SI value of greater than 0.3 represents mild, and greater than 0.5 severe SVD [10]. The mean SI was 0.35 in TLE and significantly higher than controls (NEC 0.31, EPC 0.28; $p < 0.001$, Fig. 2L). The SI was not higher in three TLE patients with identified cerebrovascular disease risk factors (hypertension and/or Type 1 diabetes) than those without. Mean vessel diameters and PVS were lower in TLE than control groups but not the ratio between these values (Fig. 2M-O).

Vascular size, types, and densities

The median diameter of COL4 vessels was lower in TLE across all white matter ROI compared to control groups ($p < 0.05$ to 0.0001 , Supp Table 2, Fig. 2P). COL4 and SMA vascular densities were both significantly higher in TLE than NEC in the MTG core but not other ROI ($p < 0.005$, $p < 0.05$, Mann Whitney test) (Supplemental Fig. 6A,B, Suppl Table 2). Classification of different vessel sizes quantified on PDGFR β , showed greater differences in the deep than core regions in TLE than NEC, including higher capillary and arteriole densities in the MTGD (Mann Whitney, $p < 0.05$, Supplemental Fig. 6C). These findings support reduced mean size of small vessels in TLE, but without a uniform increase in small vessel densities across white matter ROI.

Pericyte distribution

SMA + and PDGFR β + vessels were classified as type 1 or 2 based on complete or incomplete vascular coverage respectively. In TLE, PDGFR β type 1 vessel densities were significantly greater, whereas type 2 PDGFR β vessel densities were lower in deep white matter ROI in TLE compared to controls ($p = 0.015$ to $p = 0.009$) (Supplemental Fig. 6D,F, Supplemental Table 2); significant differences were not observed with SMA however (Supplemental Fig. 6H,J). There was evidence that Type 2 vessel were smaller in TLE than control groups in some ROI (SMA STGC $p < 0.05$; SMA MTGD $p < 0.001$; PDGFR β STGD $p < 0.05$) whereas type 1 vessel diameters were larger than controls (PDGFR β MTGC $p = 0.04$, STGD $p = 0.04$, MTGD $p = 0.001$) (Supplemental Fig. 6E,G,I,K). Paired tests showed significantly greater difference between type 1 and 2 vessels size with SMA in TLE cases than controls ($p < 0.001$ all ROI, Fig. 2Q). Analysis of double labelling for SMA and PDGFR β showed higher densities of PDGFR β + /SMA + and PDGFR β + /SMA- in TLE than controls, reaching significance for type 2 vessels in the deep white matter ($p = 0.028$, Figure Supplemental Fig. 6I). These findings support increased pericyte vascular coverage of small vessels as well as altered relative expression of PDGFR β and SMA in capillary pericytes in TLE.

Comparisons of gyral core to deep white matter

We further explored differences between gyral core and deep white matter for pathology variables, comparing average values across all gyri in TLE (Fig. 3) and control groups (Supplemental Fig. 7A,B). PLP LI was higher in the core than deep WM in TLE ($p < 0.001$) and controls ($p < 0.05$). For glial cells both Iba1 and PDGFR β LI were increased in the deep white matter in TLE ($p < 0.01$) but no differences noted in controls whereas OLIG2

showed a core > deep gradient in control groups only ($p < 0.05$). For small vessels, notable findings were that type 1 vessel densities were higher in the deep than core white matter (for SMA and PDGFR β ($p < 0.01$)) with an opposite gradient noted in controls ($p < 0.05$). In contrast PDGFR β type 2 vessel densities were higher in the core white matter in TLE ($p < 0.001$) with no differences in controls. These observations highlight a superficial to deep white matter gradients for glio-vascular pathology in TLE which differs to controls.

Within both core and deep white matter, correlations between the vascular morphometric measures and glial/myelination were observed in TLE (Supplemental Fig. 7C,D). For example, SI positively correlated with PDGFRB glia and negatively with axonal neurofilament in the deep white matter. PVS negatively correlated with core PLP. Further correlations between glial, microglia, matrix protein Tenascin-C and small vessel densities suggest interactions in TLE.

RNA expression data in TLE

Epilepsy surgical and non-lesional postmortem cases showed clustering of cases into three groups with one group enriched with surgical cases (Fig. 1Za). 135 genes showed at least one-fold significant difference between postmortem and surgical cases (unadjusted $P < 0.05$, 40 genes when using Benjamini-Hochberg adjusted P value, $P < 0.05$, Fig. 1Zb), and bioinformatic analysis using Reactome revealed that these genes were associated with Developmental Biology and Signaling Transduction pathways including EGR2 and SOX10-mediated initiation of myelination and signaling by VEGF. Genes of interest associated with myelination and oligodendroglia including MAG, PLLP (proteolipid plasmolipin) and Olig2 showed significantly reduced mRNA expression in postmortem cases compared with surgical cases ($p < 0.001$), whereas PDGFR β revealed higher gene expression in postmortem cases compared with surgical cases ($p < 0.001$) (Fig. 1Zc).

Pathology and RNA expression in HS cases

Most cases had HS (33/44), but we did not observe significant differences between mean core and deep white matter pathology variables in the fewer cases without HS apart from PDGFR β type 1 vessels which had increased diameter and reduced PLP in core regions in HS ($p \leq 0.05$) (Supplemental Fig. 8A). Gene expression analysis however showed more significant findings with reduced MAG, PLLP and Olig2 in HS compared to non-lesional epilepsy surgical cases ($p < 0.05$, Supplemental Fig. 8B,C) in addition to genes known to interact with MAG such as MBP, SOX10 ($P < 0.05$) and NGFR ($P < 0.05$) according to STRING database [65]. MAG expression and genes in myelination pathway positively associated with genes in the angiogenesis and activated microglia and cytokines pathways but with greater correlation in non-HS cases (Supplemental Fig. 8D-H). These findings support evidence for a relatively greater reduction of myelination in HS/TLE and interaction of myelination, angiogenesis pathways and neuroinflammation in non-HS cases.

DWI metrics in relation to white matter pathology: DWI measures showed regional differences in TLE with RD values higher in the gyral cores than deep white matter whereas AD, MD, FA and FIXEL were higher in the deep regions (Fig. 3). Linear regression analysis of DWI values with pathology variables revealed greater significance in core than deep white matter regions (Supplemental Table 3). Glial labelling (Iba1 and PDGFR β) increased with higher diffusion parameters (AD, RD and MD, $p < 0.05$ to < 0.0001) and higher myelin (PLP) labelling with lower AD ($p < 0.05$) and FA values in the core (Fig. 4A-D). Regarding vasculature, type 2 vessel density regressed with FA and FIXEL measures in the core white matter: higher PDGFR β and SMA with lower FA and

greater FIXEL respectively ($p < 0.05$) Fig. 4E,F). In the deep white matter, greater mean PVS associated with lower FA (Fig. 4G). In addition COL4 vessel diameters positively correlated with MD and AD in both core and deep white matter (Fig. 4H,I). These observations suggest that although DWI differences between core and deep white matter may partly be explained by anatomical differences in axon bundle organisation, alterations of glial density and vascular structures in TLE further influence diffusion measures (Figure. 5G). In the ten cases with paired DWI and gene-expression data from deep white matter, positive association between myelination genes (MOG, MAG, MBP, PLLP) and FA and negative relationship with RD was noted (Supplemental Table 3).

White matter pathology and neuropsychometry

Nine of 43 patients were classified as having verbal decline in cognitive function pre-operatively and 9/43 with impaired working memory at the time of surgery. Using logistic regression analysis for mean deep and core white matter values for groups with or without cognitive decline, we found higher PVS measure (Fig. 5A) and SMA type 2 vessel densities (Fig. 5B) in the decline group, as well as reduced vascular diameters for deep type 1 vessels (SMA and PDGFR β) and type 2 vessels in core and deep (PDGFR β) (Fig. 5C-F). There was also a trend for lower MAG LI (Supplemental Table 5). There were no significant relationships for pathology variables and impaired working memory impairment at the time of surgery. These findings support a relationship between microvascular alterations, including vessel calibre in those patients with TLE who have declined in their general verbal intellect over time prior to surgery.

White matter pathology and epilepsy history

A positive correlation between age and SI was noted in the post-mortem controls only (Spearman's $r = 0.594$). There was no correlation between SI or PVS and duration of epilepsy in the TLE group but small vessel measurements were more abnormal the longer the epilepsy, including increased vascular diameter (SMA, $p < 0.05$) and reduced vascular density (COL4, $p < 0.05$) in the core white matter (Supplemental Fig. 9A,D). Regarding vessel types, type 1 vessel densities increased with age whereas type 2 vessels decreased with duration of epilepsy (PDGFR β , Deep; $p < 0.05$) (Supplemental Fig. 9C,F). In addition, reduced axonal labelling was observed with age (NF-M, Deep ; $p < 0.05$) and more pronounced the longer the epilepsy (NF-H, Deep; $p < 0.01$) (Supplemental Fig. 9B,E). There were no differences for vascular, glia axonal or myelin markers in relation to hemisphere side. Gene expression of MAG, PLLP, Olig2 and PDGFR β was compared between patients with an age of surgery lower or equal to 40 years and over 40 years of age; the older cohort showed lower expression of MAG, PLLP, OLIG2 mRNA whereas PDGFR β RNA level appeared to be slightly higher (Supplemental Fig. 9D). These findings suggest that longer duration of epilepsy is associated with age-related alterations of myelin and microvasculature changes.

Discussion

White matter vessel disease in TLE is of relevance through its impact on brain perfusion, myelin integrity and ultimately, cognitive function. In this morphometric and transcriptomic study, we identified alterations to white matter vessels, including degenerative sclerosis and altered distribution of vascular pericytes compared to controls with differences noted between core and deep white matter. Furthermore, vascular changes correlated

with MRI measures of white matter integrity (DWI and FBA), duration of epilepsy and cognitive decline supporting dynamic changes of clinical importance.

Small vessel degenerative microangiopathy in TLE

There is growing evidence that microvascular dysfunction occurs in epilepsy and is detrimental to both seizure control and its comorbidities [47, 51] but is a relatively under investigated area in surgical series. An early study showed that SVD characterized by increased wall thickness of capillaries occurred in spiking areas [37] and a 'spongiform angiopathy' of the white matter was reported in young patients, with spitting of the vascular basement membrane and enlargement of the PVS [25]. In our series of adult TLE cases we identified a mild increase in small vessel hyaline arteriosclerosis in TLE supported by an elevated mean sclerotic index, a standard morphometric measure used for degenerative SVD in aging and dementia [7]. This was compared to control groups, which included both non-epilepsy patients (with an older mean age) and non-TLE epilepsy controls. We included an epilepsy control group without focal brain lesions or TLE to identify any epilepsy-related pathology, and for some markers, as PLP and glial markers, measurements were intermediate between TLE and non-epilepsy cases. Of note, a relationship between age and sclerotic index was lacking in the TLE group, suggesting age-independent mechanisms for the SVD. Subtypes of brain arteriosclerosis with different causes, including genetic, metabolic and hemodynamics are recognised [7]. It is plausible that repetitive vascular dysfunction, including BBB disturbances following seizures [57], is a contributing factor in TLE and inter-ictal BBB dysfunction recently correlated with memory dysfunction [52]. We also noted splitting of the basement membrane on COL4 stain in TLE cases and prominent PVS, the latter shown to be a predictor of cognitive impairment in vascular dementia [7, 27]. In addition, SI and increased PVS correlated with reduced white matter myelin and axonal labelling which may imply tissue perfusion impairment. PVS enlargement also correlated with pre-operative cognitive decline as well as reduced white matter FA on DWI, indicating clinical and imaging relevance of this degenerative feature. However, we did not observe increased PVS compared to post-mortem controls, which may be explained by agonal retardation of interstitial fluid clearance. The PVS is part of the CNS glymphatic system [74] and failure of this system for metabolite clearance is implicated in neurodegeneration [72]. Accumulation of perivascular corpora amylacea (also called 'wasteosomes') and pigment-laden macrophages is a common observation in TLE [54] as in the present series, in support of impaired periarterial drainage. Recent studies also showed ipsilateral glymphatic dysfunction in TLE with DTI-ALPS imaging [79] warranting further in-depth study of these processes in relation to clinical and cognitive impairment in epilepsy.

Small vessel regenerative microangiopathy in TLE

In the present study, white matter RNA expression analysis showed an increase in angiogenesis pathways. Using COL4, SMA and PDGFRB vascular markers, there was some evidence to support a quantitative increase in vascular density in TLE cases, although noting this was neither uniform nor a consistent pattern through white matter regions. Furthermore, as it was not feasible to calculate the absolute number of vessels, we cannot exclude that our quantitative data partly reflect regional reduced white matter volume than a real increase in small vessel number. There is controversy if angiogenesis occurs in TLE-HS. Increased vessel number was reported in the hippocampus in TLE patients [55] but not in other studies [2] and there is limited data on cortical or white vasculature (recently reviewed in [69]). Enhanced angiogenesis was shown using proteomic analysis of epileptogenic cortex [29] and quantification of vessels using CD34 endothelial marker in

a range of focal malformations noted a correlation between grey matter vascular density and epilepsy duration, but not in white matter [71].

We noted more consistent evidence for a reduction in small vessel size in TLE white matter with all markers (COL4, SMA and PDGFR β) and increased pericyte coverage. Vascular caliber and contractility are relevant to white matter perfusion and dependent on contractile vascular smooth muscle cells and pericytes. Higher pericyte to endothelial ratios occur in the cerebral vasculature, considered essential for BBB integrity and to regulate local blood flow for neurovascular coupling [1]. There is experimental evidence of dynamic changes to pericytes in epilepsy; pericytes show microscopic vasoconstrictions following seizures in animal models [34]. In spiking areas in surgical samples, degeneration of pericytes was noted compared to non-spiking regions [37]. Following status epilepticus in models, initial loss of perivascular cells was followed by an increased turnover with redistribution of PDGFR β + along vessels [3, 40]. In slice cultures, pericyte injury following induced seizures was associated with neurovascular decoupling, BBB impairment and irreversible vascular constriction [47] and interestingly smaller vessel diameters was observed with increased pericyte number [3].

Morphological diversity of pericytes is recognized; 'ensheathing' pericytes cover 95% of the endothelial surface in first branch capillaries, whereas mesh and strand pericytes on downstream capillaries have less complete coverage [21, 61, 78]. Ensheathing pericytes between arterioles and first branch capillaries were shown to strongly express SMA and act as pre-capillary sphincters, regulating local capillary blood flow [78] whereas there is reduced SMA gene expression in distal mesh and strand pericytes [21]. In the current study we classified type 1 or 2 vessels based on complete or incomplete circumferential coverage of pericytes as we were quantifying on thin sections with vessels in random directions. We observed increased type 1 and reduced type 2 vessels, particularly in the deep white matter in TLE than controls with PDGFR β , in support of increased pericyte vessel coverage. In addition, SMA was noted in smaller vessels compared to controls, supporting increased capillary contractile function. Pericyte vessel coverage was increased with longer duration of epilepsy supporting this could be an acquired dynamic process. One interpretation of the altered relative expression of SMA to PDGFR β in pericytes together with overall smaller vessel coverage, is a functional alteration of contractility which could impact on haemodynamic regulation and white matter perfusion [21]. Of note, our observation is the opposite to findings in SVD associated with aging and dementia where loss and degeneration of pericytes occurs (reviewed in [67]). In addition, we also noted a relationship between reduced vascular size and cognitive impairment supporting the potential relevance of this TLE-related SVD warranting further investigation in larger cohorts.

Diffusion MRI and superficial white matter vascular pathology

DWI alterations are common in TLE [24] although few studies report pathology correlations [12, 20, 38]. Reduced FA and increased MD in the temporal lobe and pole in TLE [36, 75] has been interpreted to reflect degradation of myelin sheaths, reduced axonal number, increased extra-axonal space and reactive astrogliosis [9, 23, 75]. It is recognised that white matter small vessel disease may result in diffuse changes to FA and MD in epilepsy (Wang, Zuo et al. 2024) but there have not been focused investigation in TLE. Previous DWI studies in TLE have also reported specific superficial white matter abnormalities [36, 68] related to network dysfunction, memory impairment [77] and cognitive phenotype [53].

We noted more frequent correlations between diffusivity in the core white matter and, furthermore, with vascular size and glial density (PDGFR β and Iba1) than myelin markers. An inverse correlation between FA and PLP in the core may reflect a preferential dysmyelination in projection white matter fibres. FBA is a recent DWI tool that renders a measure of both white matter fibre distribution and orientation in addition to density [13] and has been noted to discriminate white matter alterations in TLE from other epilepsies [42]. Such methods are relevant to analysis of superficial temporal lobe white matter with different directionality of crossing 'U' and radial projection fibres, and reflected in the gradient we observed in DWI measures between core and deep compartments. Correlations between FA/FIXEL and vascular density and PVS support that degenerative vascular disease can impact on diffusion metrics. This highlights the influence of vascular pathology, through either direct or its indirect effects on other white matter structures, to diffusion imaging.

The increased parenchymal PDGFR β cells in TLE was a striking finding and previously reported in focal epilepsy [19, 40, 59] and they may represent a NG-2 glial progenitor type. Their biological roles as a source of new pericytes and contribution to CNS scarring and vascular sclerosis is of ongoing interest [26, 31, 50] and we noted a correlation with vascular sclerosis in this cohort. Of note, despite immunohistochemical evidence of increased parenchymal and perivascular PDGFR β + cells in TLE, bulk RNA transcripts of white matter showed lower expression than controls. The PDGFR β signaling pathway is critical to developmental angiogenesis and recent evidence confirms roles in ongoing maintenance of pericytes in the adult brain [70] where a complex process of receptor internalization and signal attenuation is shown to fine tune PDGFR activity and responses [56]. Such sequestration may explain the discordance in our findings between gene and cellular expression in TLE and highlights the need for single cell analysis to explore any alterations in this signaling pathway in epilepsy. Indeed, altered PDGFR β signaling with loss of pericytes has been identified in AD as a potential therapeutic target [60] and the loss of PDGFR β + white matter pericytes in post-stroke dementia [14, 17].

Myelin and oligodendroglia in TLE

Alteration to white matter axonal myelination is recognised in epilepsy with evidence for both a reduction [16, 45] and increase [33]. Differences in myelination dynamics between epilepsies may be reflect neuronal and network activity, oligodendrogliosis, neuroinflammation but also tissue hypoperfusion [32]. White matter myelination has been more comprehensively investigated in focal cortical dysplasia [11] with reduced myelin [59] and downregulation of myelin-associated transcripts in the dysplastic region (Donkels 2017), possibly driven by mTOR effects on oligodendroglia [22]. In TLE, a reduction in white matter, projection myelinated axons and increased extra-axonal space has been reported [9, 20, 45]. We also noted greater myelin transcript reduction in HS than non-HS cases and with increasing age at surgery.

Previous quantitative studies of white matter myelination in TLE utilized tinctorial stains or myelin basic protein (MBP) [20, 38]. We studied MAG, which is highly susceptible to reduced tissue oxygenation and PLP a more resistant myelin protein ; these comparative markers have been used in post-mortem studies as indirect measures of white matter hypoperfusion in vascular dementia [41] and may reflect dynamic changes to myelin. We noted a reduction of MAG, and to a lesser extent PLP, compared to non-epilepsy controls, particularly in deep white matter in TLE. One interpretation is that a progressive degeneration of projection white matter fibers occurs and episodic tissue hypoperfusion in seizures may be an influencing factor. In contrast, however, tissue transcripts of white matter myelination genes were increased which likely reflect the observed oligodendrogliosis. White matter oligodendrogliosis is long recognized in focal and experimental epilepsy

including TLE [28, 33, 58, 62] although the cause and functional significance remains unclear. Recently oligodendroglia hyperplasia in frontal lobe epilepsy has been linked with deficient white matter myelination and *SLC35A2* brain mosaicism (MOGHE) [8]. Further understanding of any maladaptive or dysfunctional myelination arising in TLE, and vascular versus genetic causes, is needed as it may both exacerbate seizures and impair optimal neurological function [32].

Limitations of the study

Although we selected control cases with shortest post-mortem intervals and fixation times, we cannot exclude that tissue handling factors between surgical TLE samples and agonal changes influence pathology and vascular measures. In some ROIs there was missing pathology data due to technical and tissue quality reasons. The subsets with cognitive decline were relatively small in this cohort which was selected primarily on availability of DWI. Still, our findings suggest that the pathological changes observed are related to the decline of cognitive functioning rather than explaining impairment detected prior to surgery, which is likely multi-factorial, including the effects of medication and seizure frequency. Future similar studies are essential with larger case numbers with cognitive decline to validate the relative contribution of SVD pathology compared to other degenerative and acquired processes.

Conclusions

In summary, mild age-independent small vessel arteriolosclerosis coupled with altered distribution of white matter pericytes and increased extension to smallest vessels represent acquired and adaptive alterations in TLE and have potential haemodynamic influences on white matter myelination, glial proliferation, MRI diffusion alterations and consequently, might explain cognitive decline. Further investigations in larger cohorts paralleled with other neurodegenerative and cortical pathology markers and genetic risk factors for neurodegenerative and vascular disease is the next step.

Declarations

Acknowledgements

We are grateful to the assistance of Maritchka Ryniejska, supported by the Epilepsy Society Brain and Tissue Bank for help with sample preparation, immunostaining and scanning and also to UCL students Eugenia Belen Dri Rios, Ankith Mannath, Cuiting Zhang, Feeza Patel for their additional help. We are grateful to the Edinburgh MRC brain and tissue bank for provision of control materials as detailed in text. We acknowledge Gavin Winston for the DWI data acquisition for controls, which was supported by the Medical Research Council (G0802012, MR/M00841X/1). We thank Beate Diehl for provision of DWI data supported through NIH—National Institute of Neurological Disorders and Stroke U01-NS090407, The Center for SUDEP Research).

Disclosure statement / Competing Interests

The authors report no competing interests

Author contributions

JL gene expression analysis; LB, FX, RM, MK, JD, all MRI data acquisitions and analysis; IP & SB neuropsychometry data analysis; SP, YL, MT, AM histology and quantitative analysis, SPan Statistical advice; JdT clinical data collection; MT, MK study design; all authors contributed to the manuscript preparation and final version.

Compliance with ethical standards

This project has ethical approval through the ESBTB (NHS research ethics committee number 23/SC/0002) with patients consented for use of human tissue in research.

Data availability statement

Summary data is presented in supplemental files and original data available on request

References

1. Alarcon-Martinez L, Yemisci M, Dalkara T (2021) Pericyte morphology and function. *Histol Histopathol* 36:633–643. [10.14670/HH-18-314](https://doi.org/10.14670/HH-18-314)
2. Alonso-Nanclares L, DeFelipe J (2014) Alterations of the microvascular network in the sclerotic hippocampus of patients with temporal lobe epilepsy. *Epilepsy Behav* 38:48–52. [10.1016/j.yebeh.2013.12.009](https://doi.org/10.1016/j.yebeh.2013.12.009)
3. Arango-Lievano M, Boussadia B, De Terdonck LDT, Gault C, Fontanaud P, Lafont C, Mollard P, Marchi N, Jeanneteau F (2018) Topographic Reorganization of Cerebrovascular Mural Cells under Seizure Conditions. *Cell Rep* 23:1045–1059. [10.1016/j.celrep.2018.03.110](https://doi.org/10.1016/j.celrep.2018.03.110)
4. Bankhead P, Loughrey MB, Fernandez JA, Dombrowski Y, McArt DG, Dunne PD, McQuaid S, Gray RT, Murray LJ, Coleman HG et al (2017) QuPath: Open source software for digital pathology image analysis. *Sci Rep* 7: 16878 [10.1038/s41598-017-17204-5](https://doi.org/10.1038/s41598-017-17204-5)
5. Baxendale S, Thompson P (2020) The association of cognitive phenotypes with postoperative outcomes after epilepsy surgery in patients with temporal lobe epilepsy. *Epilepsy Behav* 112:107386. [10.1016/j.yebeh.2020.107386](https://doi.org/10.1016/j.yebeh.2020.107386)
6. Bell B, Lin JJ, Seidenberg M, Hermann B (2011) The neurobiology of cognitive disorders in temporal lobe epilepsy. *Nat Rev Neurol* 7:154–164. [10.1038/nrneurol.2011.3](https://doi.org/10.1038/nrneurol.2011.3)
7. Blevins BL, Vinters HV, Love S, Wilcock DM, Grinberg LT, Schneider JA, Kalaria RN, Katsumata Y, Gold BT, Wang DJJ et al (2021) Brain arteriolosclerosis. *Acta Neuropathol* 141:1–24. [10.1007/s00401-020-02235-6](https://doi.org/10.1007/s00401-020-02235-6)
8. Bonduelle T, Hartlieb T, Baldassari S, Sim NS, Kim SH, Kang HC, Kobow K, Coras R, Chipaux M, Dorfmueller G et al (2021) Frequent SLC35A2 brain mosaicism in mild malformation of cortical development with oligodendroglial hyperplasia in epilepsy (MOGHE). *Acta Neuropathol Commun* 9(3). [10.1186/s40478-020-01085-3](https://doi.org/10.1186/s40478-020-01085-3)
9. Concha L, Livi DJ, Beaulieu C, Wheatley BM, Gross DW (2010) In vivo diffusion tensor imaging and histopathology of the fimbria-fornix in temporal lobe epilepsy. *J Neurosci* 30:996–1002 [Doi 10.1523/JNEUROSCI.1619-09.2010](https://doi.org/10.1523/JNEUROSCI.1619-09.2010)
10. Craggs LJ, Hagel C, Kuhlenbaeumer G, Borjesson-Hanson A, Andersen O, Viitanen M, Kalimo H, McLean CA, Slade JY, Hall RA et al et al (2013) Quantitative vascular pathology and phenotyping familial and

- sporadic cerebral small vessel diseases. *Brain Pathol* 23:547–557. 10.1111/bpa.12041
11. Deleo F, Thom M, Concha L, Bernasconi A, Bernhardt BC, Bernasconi N (2018) Histological and MRI markers of white matter damage in focal epilepsy. *Epilepsy Res* 140:29–38. 10.1016/j.epilepsyres.2017.11.010
 12. Demerath T, Donkels C, Reisert M, Heers M, Rau A, Schroter N, Schulze-Bonhage A, Reinacher P, Scheiwe C, Shah MJ al (2022) Gray-White Matter Blurring of the Temporal Pole Associated With Hippocampal Sclerosis: A Microstructural Study Involving 3 T MRI and Ultrastructural Histopathology. *Cereb Cortex* 32:1882–1893. 10.1093/cercor/bhab320
 13. Dhollander T, Clemente A, Singh M, Boonstra F, Civier O, Duque JD, Egorova N, Enticott P, Fuelscher I, Gajamange Set al et al (2021) Fixel-based Analysis of Diffusion MRI: Methods, Applications, Challenges and Opportunities. *NeuroImage* 241:118417. 10.1016/j.neuroimage.2021.118417
 14. Ding R, Hase Y, Ameen-Ali KE, Ndung'u M, Stevenson W, Barsby J, Gourlay R, Akinyemi T, Akinyemi R, Uemura MT et al (2020) Loss of capillary pericytes and the blood-brain barrier in white matter in poststroke and vascular dementias and Alzheimer's disease. *Brain Pathol* 30: 1087–1101 10.1111/bpa.12888
 15. Doerrfuss JI, Hebel JM, Holtkamp M (2023) Epileptogenicity of white matter lesions in cerebral small vessel disease: a systematic review and meta-analysis. *J Neurol* 270:4890–4902. 10.1007/s00415-023-11828-6
 16. Drenthen GS, Backes WH, Aldenkamp AP, Vermeulen RJ, Klinkenberg S, Jansen JFA (2020) On the merits of non-invasive myelin imaging in epilepsy, a literature review. *J Neurosci Methods* 338:108687. 10.1016/j.jneumeth.2020.108687
 17. Fang C, Magaki SD, Kim RC, Kalaria RN, Vinters HV, Fisher M (2023) Arteriolar neuropathology in cerebral microvascular disease. *Neuropathol Appl Neurobiol* 49:e12875. 10.1111/nan.12875
 18. Fischl B (2012) *FreeSurfer Neuroimage* 62:774–781. 10.1016/j.neuroimage.2012.01.021
 19. Garbelli R, de Bock F, Medici V, Rousset MC, Villani F, Boussadia B, Arango-Lievano M, Jeanneteau F, Daneman R, Bartolomei F, Marchi N (2015) PDGFRbeta(+) cells in human and experimental neuro-vascular dysplasia and seizures. *Neuroscience* 306:18–27. 10.1016/j.neuroscience.2015.07.090
 20. Garbelli R, Milesi G, Medici V, Villani F, Didato G, Deleo F, D'Incerti L, Morbin M, Mazzoleni G, Giovagnoli A Ret al et al (2012) Blurring in patients with temporal lobe epilepsy: clinical, high-field imaging and ultrastructural study. *Brain* 135:2337–2349. 10.1093/brain/aws149
 21. Gonzales AL, Klug NR, Moshkforoush A, Lee JC, Lee FK, Shui B, Tsoukias NM, Kotlikoff MI, Hill-Eubanks D, Nelson MT (2020) Contractile pericytes determine the direction of blood flow at capillary junctions. *Proc Natl Acad Sci U S A* 117:27022–27033. 10.1073/pnas.1922755117
 22. Gruber VE, Lang J, Endmayr V, Diehm R, Pimpel B, Glatter S, Anink JJ, Bongaarts A, Luinenburg MJ Reinten RJ (2021) Impaired myelin production due to an intrinsic failure of oligodendrocytes in mTORopathies. *Neuropathol Appl Neurobiol* 47: 812–825 10.1111/nan.12744
 23. Hatton SN, Huynh KH, Bonilha L, Abela E, Alhusaini S, Altmann A, Alvim MKM, Balachandra AR, Bartolini E, Bender Bet al et al (2020) White matter abnormalities across different epilepsy syndromes in adults: an ENIGMA-Epilepsy study. *Brain* 143:2454–2473. 10.1093/brain/awaa200
 24. Hatton SN, Huynh KH, Bonilha L, Abela E, Alhusaini S, Altmann A, Alvim MKM, Balachandra AR, Bartolini E, Bender Bet al et al (2020) White matter abnormalities across different epilepsy syndromes in adults: an

ENIGMA-Epilepsy study. *Brain*: 10.1093/brain/awaa200

25. Hildebrandt M, Amann K, Schroder R, Pieper T, Kolodziejczyk D, Holthausen H, Buchfelder M, Stefan H, Blumcke I (2008) White matter angiopathy is common in pediatric patients with intractable focal epilepsies. *Epilepsia* 49:804–815. 10.1111/j.1528-1167.2007.01514.x
26. Hirunpattarasilp C, Attwell D, Freitas F (2019) The role of pericytes in brain disorders: from the periphery to the brain. *J Neurochem* 150:648–665. 10.1111/jnc.14725
27. Kalaria RN (2018) The pathology and pathophysiology of vascular dementia. *Neuropharmacology* 134:226–239. 10.1016/j.neuropharm.2017.12.030
28. Kasper BS, Paulus W (2004) Perivascular clustering in temporal lobe epilepsy: oligodendroglial cells of unknown function. *Acta Neuropathol* 108:471–475. 10.1007/s00401-004-0914-3
29. Keren-Aviram G, Dachet F, Bagla S, Balan K, Loeb JA, Dratz EA (2018) Proteomic analysis of human epileptic neocortex predicts vascular and glial changes in epileptic regions. *PLoS ONE* 13:e0195639. 10.1371/journal.pone.0195639
30. Kim HW, Hong J, Jeon JC (2020) Cerebral Small Vessel Disease and Alzheimer's Disease: A Review. *Front Neurol* 11:927. 10.3389/fneur.2020.00927
31. Klement W, Blaquiére M, Zub E, deBock F, Boux F, Barbier E, Audinat E, Lerner-Natoli M, Marchi N (2019) A pericyte-glia scarring develops at the leaky capillaries in the hippocampus during seizure activity. *Epilepsia* 60:1399–1411. 10.1111/epi.16019
32. Knowles JK, Batra A, Xu H, Monje M (2022) Adaptive and maladaptive myelination in health and disease. *Nat Rev Neurol* 18:735–746. 10.1038/s41582-022-00737-3
33. Knowles JK, Xu H, Soane C, Batra A, Saucedo T, Frost E, Tam LT, Fraga D, Ni L, Villar Ket al et al (2022) Maladaptive myelination promotes generalized epilepsy progression. *Nat Neurosci* 25:596–606. 10.1038/s41593-022-01052-2
34. Leal-Campanario R, Alarcon-Martinez L, Rieiro H, Martinez-Conde S, Alarcon-Martinez T, Zhao X, LaMee J, Popp PJ, Calhoun ME, Arribas JI et al (2017) Abnormal Capillary Vasodynamics Contribute to Ictal Neurodegeneration in Epilepsy. *Sci Rep* 7: 43276 10.1038/srep43276
35. Li Y, Liu P, Lin Q, Zhou D, An D (2023) Postoperative seizure and memory outcome of temporal lobe epilepsy with hippocampal sclerosis: A systematic review. *Epilepsia* 64:2845–2860. 10.1111/epi.17757
36. Liu M, Bernhardt BC, Hong SJ, Caldairou B, Bernasconi A, Bernasconi N (2016) The superficial white matter in temporal lobe epilepsy: a key link between structural and functional network disruptions. *Brain* 139:2431–2440. 10.1093/brain/aww167
37. Liwnicz BH, Leach JL, Yeh HS, Privitera M (1990) Pericyte degeneration and thickening of basement membranes of cerebral microvessels in complex partial seizures: electron microscopic study of surgically removed tissue. *Neurosurgery* 26:409–420. 10.1097/00006123-199003000-00006
38. Lockwood-Estrin G, Thom M, Focke NK, Symms MR, Martinian L, Sisodiya SM, Duncan JS, Eriksson SH (2012) Correlating 3T MRI and histopathology in patients undergoing epilepsy surgery. *J Neurosci Methods* 205:182–189. 10.1016/j.jneumeth.2011.12.014
39. Marchi N, Lerner-Natoli M (2013) Cerebrovascular remodeling and epilepsy. *Neuroscientist* 19:304–312 Doi 10.1177/1073858412462747

40. Milesi S, Boussadia B, Plaud C, Catteau M, Rousset MC, De Bock F, Schaeffer M, Lerner-Natoli M, Rigau V, Marchi N (2014) Redistribution of PDGFRbeta cells and NG2DsRed pericytes at the cerebrovasculature after status epilepticus. *Neurobiol Dis* 71:151–158. 10.1016/j.nbd.2014.07.010
41. Miners JS, Palmer JC, Love S (2016) Pathophysiology of Hypoperfusion of the Precuneus in Early Alzheimer's Disease. *Brain Pathol* 26:533–541. 10.1111/bpa.12331
42. Mito R, Pedersen M, Pardoe H, Parker D, Smith RE, Cameron J, Scheffer IE, Berkovic SF, Vaughan DN, Jackson GD (2024) Exploring individual fixel-based white matter abnormalities in epilepsy. *Brain Commun* 6:fcad352. 10.1093/braincomms/fcad352
43. O'Brien JT, Thomas A (2015) Vascular dementia. *Lancet* 386:1698–1706 Doi 10.1016/S0140-6736(15)00463-8
44. Ohi K, Sumiyoshi C, Fujino H, Yasuda Y, Yamamori H, Fujimoto M, Sumiyoshi T, Hashimoto R (2017) A Brief Assessment of Intelligence Decline in Schizophrenia As Represented by the Difference between Current and Premorbid Intellectual Quotient. *Front Psychiatry* 8:293. 10.3389/fpsy.2017.00293
45. Ozdogmus O, Cavdar S, Ersoy Y, Ercan F, Uzun I (2009) A preliminary study, using electron and light-microscopic methods, of axon numbers in the fornix in autopsies of patients with temporal lobe epilepsy. *Anat Sci Int* 84:2–6. 10.1007/s12565-008-0001-2
46. Pachitariu M, Stringer C (2022) Cellpose 2.0: how to train your own model. *Nat Methods* 19:1634–1641. 10.1038/s41592-022-01663-4
47. Prager O, Kamintsky L, Hasam-Henderson LA, Schoknecht K, Wuntke V, Papageorgiou I, Swolinsky J, Muoio V, Bar-Klein G, Vazana U (2019) Seizure-induced microvascular injury is associated with impaired neurovascular coupling and blood-brain barrier dysfunction. *Epilepsia* 60: 322–336 10.1111/epi.14631
48. Raffelt DA, Smith RE, Ridgway GR, Tournier JD, Vaughan DN, Rose S, Henderson R, Connelly A (2015) Connectivity-based fixel enhancement: Whole-brain statistical analysis of diffusion MRI measures in the presence of crossing fibres. *NeuroImage* 117:40–55. 10.1016/j.neuroimage.2015.05.039
49. Raffelt DA, Tournier JD, Smith RE, Vaughan DN, Jackson G, Ridgway GR, Connelly A (2017) Investigating white matter fibre density and morphology using fixel-based analysis. *NeuroImage* 144:58–73. 10.1016/j.neuroimage.2016.09.029
50. Reeves C, Pradim-Jardim A, Sisodiya SM, Thom M, Liu JYW (2019) Spatiotemporal dynamics of PDGFRbeta expression in pericytes and glial scar formation in penetrating brain injuries in adults. *Neuropathol Appl Neurobiol* 45:609–627. 10.1111/nan.12539
51. Reiss Y, Bauer S, David B, Devraj K, Fidan E, Hattingen E, Liebner S, Melzer N, Meuth SG, Rosenow F et al (2023) The neurovasculature as a target in temporal lobe epilepsy. *Brain Pathol* 33:e13147. 10.1111/bpa.13147
52. Reiter JT, Schulte F, Bauer T, David B, Endler C, Isaak A, Schuch F, Bitzer F, Witt JA, Hattingen E (2024) Evidence for interictal blood-brain barrier dysfunction in people with epilepsy. *Epilepsia* 65: 1462–1474 10.1111/epi.17929
53. Reyes A, Kaestner E, Bahrami N, Balachandra A, Hegde M, Paul BM, Hermann B, McDonald CR (2019) Cognitive phenotypes in temporal lobe epilepsy are associated with distinct patterns of white matter network abnormalities. *Neurology* 92: e1957-e1968 10.1212/WNL.00000000000007370

54. Riba M, Del Valle J, Molina-Porcel L, Pelegri C, Vilaplana J (2022) Wasteosomes (corpora amylacea) as a hallmark of chronic glymphatic insufficiency. *Proc Natl Acad Sci U S A* 119:e2211326119. 10.1073/pnas.2211326119
55. Rigau V, Morin M, Rousset MC, de Bock F, Lebrun A, Coubes P, Picot MC, Baldy-Moulinier M, Bockaert J, Crespel A, Lerner-Natoli M (2007) Angiogenesis is associated with blood-brain barrier permeability in temporal lobe epilepsy. *Brain* 130:1942–1956. 10.1093/brain/awm118
56. Rogers MA, Fantauzzo KA (2020) The emerging complexity of PDGFRs: activation, internalization and signal attenuation. *Biochem Soc Trans* 48:1167–1176. 10.1042/BST20200004
57. Ruber T, David B, Luchters G, Nass RD, Friedman A, Surges R, Stocker T, Weber B, Deichmann R, Schlaug G et al (2018) Evidence for peri-ictal blood-brain barrier dysfunction in patients with epilepsy. *Brain* 141: 2952–2965 10.1093/brain/awy242
58. Sakuma S, Halliday WC, Nomura R, Ochi A, Otsubo H (2014) Increased population of oligodendroglia-like cells in pediatric intractable epilepsy. *Neurosci Lett* 566:188–193. 10.1016/j.neulet.2014.03.002
59. Shepherd C, Liu J, Goc J, Martinian L, Jacques TS, Sisodiya SM, Thom M (2013) A quantitative study of white matter hypomyelination and oligodendroglial maturation in focal cortical dysplasia type II. *Epilepsia* 54:898–908. 10.1111/epi.12143
60. Smyth LCD, Hight B, Jansson D, Wu J, Rustenhoven J, Aalderink M, Tan A, Li S, Johnson R Coppieters N (2022) Characterisation of PDGF-BB:PDGFRbeta signalling pathways in human brain pericytes: evidence of disruption in Alzheimer's disease. *Commun Biol* 5: 235 10.1038/s42003-022-03180-8
61. Smyth LCD, Rustenhoven J, Scotter EL, Schweder P, Faull RLM, Park TIH, Dragunow M (2018) Markers for human brain pericytes and smooth muscle cells. *J Chem Neuroanat* 92:48–60. 10.1016/j.jchemneu.2018.06.001
62. Stefanits H, Czech T, Pataria E, Baumgartner C, Derhaschnig N, Slana A, Kovacs GG (2012) Prominent oligodendroglial response in surgical specimens of patients with temporal lobe epilepsy. *Clin Neuropathol* 31:409–417. 10.5414/np300536
63. Stringer C, Wang T, Michaelos M, Pachitariu M (2021) Cellpose: a generalist algorithm for cellular segmentation. *Nat Methods* 18:100–106. 10.1038/s41592-020-01018-x
64. Swissa E, Serlin Y, Vazana U, Prager O, Friedman A (2019) Blood-brain barrier dysfunction in status epilepticus: Mechanisms and role in epileptogenesis. *Epilepsy Behav* 101:106285. 10.1016/j.yebeh.2019.04.038
65. Szklarczyk D, Kirsch R, Koutrouli M, Nastou K, Mehryary F, Hachilif R, Gable AL, Fang T, Doncheva NT, Pyysalo S et al (2023) The STRING database in 2023: protein-protein association networks and functional enrichment analyses for any sequenced genome of interest. *Nucleic Acids Res* 51:D638–D646. 10.1093/nar/gkac1000
66. Tai XY, Koeppe M, Duncan JS, Fox N, Thompson P, Baxendale S, Liu JY, Reeves C, Michalak Z, Thom M (2016) Hyperphosphorylated tau in patients with refractory epilepsy correlates with cognitive decline: a study of temporal lobe resections. *Brain* 139:2441–2455. 10.1093/brain/aww187
67. Uemura MT, Maki T, Ihara M, Lee VMY, Trojanowski JQ (2020) Brain Microvascular Pericytes in Vascular Cognitive Impairment and Dementia. *Front Aging Neurosci* 12:80. 10.3389/fnagi.2020.00080

68. Urquia-Osorio H, Pimentel-Silva LR, Rezende TJR, Almendares-Bonilla E, Yasuda CL, Concha L, Cendes F (2022) Superficial and deep white matter diffusion abnormalities in focal epilepsies. *Epilepsia* 63:2312–2324. 10.1111/epi.17333
69. van Lanen RH, Melchers S, Hoogland G, Schijns OE, Zandvoort MAV, Haeren RH, Rijkers K (2021) Microvascular changes associated with epilepsy: A narrative review. *J Cereb Blood Flow Metab* 41:2492–2509. 10.1177/0271678X211010388
70. Vazquez-Liebanas E, Nahar K, Bertuzzi G, Keller A, Betsholtz C, Mae MA (2022) Adult-induced genetic ablation distinguishes PDGFB roles in blood-brain barrier maintenance and development. *J Cereb Blood Flow Metab* 42:264–279. 10.1177/0271678X211056395
71. Veersema TJ, de Neef A, van Scheppingen J, Ferrier CH, van Eijsden P, Gosselaar PH, van Rijen PC, Spliet WGM, Braun KPJ, Muhlebner A, Aronica E (2019) Changes in vascular density in resected tissue of 97 patients with mild malformation of cortical development, focal cortical dysplasia or TSC-related cortical tubers. *Int J Dev Neurosci* 79:96–104. 10.1016/j.ijdevneu.2019.11.003
72. Vergheze JP, Terry A, de Natale ER, Politis M (2022) Research Evidence of the Role of the Glymphatic System and Its Potential Pharmacological Modulation in Neurodegenerative Diseases. *J Clin Med* 11. 10.3390/jcm11236964
73. Wang Y, Zuo H, Li W, Wu X, Zhou F, Chen X, Liu F, Xi Z (2024) Cerebral small vessel disease increases risk for epilepsy: a Mendelian randomization study. *Neurol Sci* 45:2171–2180. 10.1007/s10072-023-07221-w
74. Wardlaw JM, Benveniste H, Nedergaard M, Zlokovic BV, Mestre H, Lee H, Doubal FN, Brown R, Ramirez J, MacIntosh BJ al (2020) Perivascular spaces in the brain: anatomy, physiology and pathology. *Nat Rev Neurol* 16:137–153. 10.1038/s41582-020-0312-z
75. Winston GP, Vos SB, Caldairou B, Hong SJ, Czech M, Wood TC, Wastling SJ, Barker GJ, Bernhardt BC Bernasconi N (2020) Microstructural imaging in temporal lobe epilepsy: Diffusion imaging changes relate to reduced neurite density. *Neuroimage Clin* 26: 102231 10.1016/j.nicl.2020.102231
76. Witt JA, Coras R, Schramm J, Becker AJ, Elger CE, Blumcke I, Helmstaedter C (2015) Relevance of hippocampal integrity for memory outcome after surgical treatment of mesial temporal lobe epilepsy. *J Neurol* 262:2214–2224. 10.1007/s00415-015-7831-3
77. Xie K, Royer J, Lariviere S, Rodriguez-Cruces R, Frassle S, Cabalo DG, Ngo A, DeKraker J, Auer H, Tavakol Set al et al (2023) Atypical connectome topography and signal flow in temporal lobe epilepsy. *bioRxiv*: 10.1101/2023.05.23.541934
78. Zambach SA, Cai C, Helms HCC, Hald BO, Dong Y, Fordsmann JC, Nielsen RM, Hu J, Lonstrup M, Brodin B, Lauritzen MJ (2021) Precapillary sphincters and pericytes at first-order capillaries as key regulators for brain capillary perfusion. *Proc Natl Acad Sci U S A* 118. 10.1073/pnas.2023749118
79. Zhao X, Zhou Y, Li Y, Huang S, Zhu H, Zhou Z, Zhu S, Zhu W (2023) The asymmetry of glymphatic system dysfunction in patients with temporal lobe epilepsy: A DTI-ALPS study. *J Neuroradiol*: Doi. 10.1016/j.neurad.2023.05.009

Tables

Table 1. Summary data of the cases selected for studies.

Study	Group (N=number of cases)	Tissue types	Left : Right sides studied	Mean age at surgery or death (range) years	Mean age at onset of epilepsy (range) years	Duration of epilepsy years	Sex M : F	Period of tissue sample collection
Pathology studies	TLE-HS (N=33)	S- FFPE	21 : 12	39.4 (21-60)	12.0 (.7-37)	27.3 (4-47)	16 : 18	2003-2021
	TLE-No HS (N=11)	S- FFPE	6 : 5	37.6 (24-55)	17.3 (7-51)	20.7 (1-40)	6 : 5	2011-2019
	NEC (N=28)	PM- FFPE	25 : 25	47.5 (23-90)	N/A	N/A	15 : 13	1998-2019
	EPC (N=8)	PM- FFPE	8 : 8	29.87 (16-41)	15* (5-26)	14 (1-28)*	5 : 3	2013-2019
Gene expression studies	TLE-HS (N=16)	S-FS	8 : 8	43.8 (20-60)	14.9 (3-50)	28.8 (7-47)	6 : 10	2011-2021
	TLE-No HS (N=6)	S-FS	1 : 5	37.5 (21-50)	11.8 (12-25)	25.6 (6-40)	4 : 2	2017-2019
	FLE (non- lesional) (N=6)	S-FS	2 ; 4	35.5 (23-47)	17.1 (5-41)	18.3 (6-36)	4 : 2	2012-2015
	NEC (N=6)	PM-FS	na	43 (33- 58)	N/A	N/A	4 : 0	2014-2016
	EPC (N=6)	PM-FS	na	44 (33-57)	17.6* (1-31)	28.3* (2-47)	2 : 2	2015-2021

EPC = epilepsy controls, FLE = frontal lobe epilepsy, TLE = temporal lobe epilepsy, NEC = non-epilepsy controls, PM (post mortem), S = surgical, FS = Frozen (-70⁰C) sample, FFPE = formalin-fixed paraffin-embedded. N/A = not applicable and na=not available. *For post-mortem cases precise clinical information on age of seizure onset is missing for some cases (see supplemental Table 1). For NEC cases, all autopsies were performed within 24 hours after death and fixed in neutral buffered formalin for no more than one week. No remarkable abnormalities were observed in white matter of any cases during standard neuropathology assessment using routine histological stains and immunohistochemical panels consisting of neuronal, astrocytic and microglial markers except for one PM case which had small area of white matter scarring. Clinical records on patients' seizure history, including age of onset, seizure types (generalised convulsive, focal) and risk factors for arteriolosclerosis can be found in supplemental Table 1 for the pathology studies.

Table 2: Immunohistochemistry (IHC) panel, method and quantitative analysis conducted. Further detail on methods is available in supplementary materials files.

GROUP	IHC marker	Expression patterns; Rationale for use in study	Antibody Clone ; source ; dilution ; IHC method	Quantitative analysis
MYELIN AND AXONS	Myelin associated glycoprotein (MAG)	Type 1 transmembrane glycoprotein on the inner membrane of myelin sheaths; susceptible to reduced tissue oxygenation as marker of tissue hypoperfusion/small vessel disease [1]	Rabbit monoclonal ab277524 ; Abcam, UK ; 1:2500 ; ER2 – 20 mins; Leica Bondmax	Automated whole slide image analysis (Qupath) [2]– Labelling Index in ROI
	Phospho-lipid protein-1 (PLP)	Myelin transmembrane domain protein / binds myelin sheath and interacts with MAG ; in comparison to MAG relatively resistant to tissue hypoperfusion [1]	Rabbit polyclonal HPA004128; Cambridge Biosciences; 1: 500; ER1 – 20 mins; Leica Bondmax	Automated whole slide image analysis (Qupath) – Labelling Index in ROI
	Neurofilament Light chain (NF-L)	Type IV intermediate filament (MW 68 KDa) ; expression, phosphorylation reflects axon calibre, myelination and conduction velocity [3] ; loss may reflect axonal injury/depletion [4]	Mouse monoclonal Phosphorylated Neurofilament cocktail, DAKO/Cappel (NFC); M0762; 1:500; ER2 – 20 mins; Leica Bondmax	Automated whole slide image analysis (Qupath) – Labelling Index in ROI
	Neurofilament Medium chain (NF-M)	Type IV intermediate filament (MW 150 KDa) ; as for NF-L	Mouse monoclonal Neurofilament phosphorylation (NFP) - also reacts with HF-H; MAB1592; Merck; 1:3200; ER1 – 20 mins; Leica Bondmax	Automated whole slide image analysis (Qupath) – Labelling Index in ROI
	Neurofilament Heavy chain (NF-H)	Type IV intermediate filament (MW 190-210 KDa) ; as for NF-L	Mouse monoclonal SMI31 Phosphorylated neurofilament 801601; Sternberger/Biolgend; 1:5000; no antigen retrieval; Leica Bondmax	Automated whole slide image analysis (Qupath) – Labelling Index in ROI
GLIA AND MATRIX	Neuronal nuclear antigen (NeuN)	Mature Neuronal marker	Rabbit polyclonal ab104225; Abcam; 1:500; ER1 – 20 mins; Leica Bondmax	Qupath/cellpose for automated cell density

	Oligodendrocyte transcription factor 2 (Olig2)	Oligodendroglial lineage marker	Mouse monoclonal MABN50 211F1.1; Sigma Aldrich; 1:400; ER2 – 20 mins; Leica Bondmax	Qupath/cellpose for automated cell density
	Ionized calcium-binding adaptor molecule 1 (Iba1)	Resting and activated microglia	Rabbit polyclonal 019-19741; Fujifilm WAKO; 1:1000; ER2-30 mins; Leica Bondmax	Automated whole slide image analysis (Qupath) – Labelling Index in ROI
	Tenascin C	Extracellular matrix protein ; roles in tissue repair, upregulated in gliosis and angiogenesis and experimental epilepsy [5]	Rabbit monoclonal ab108930; Abcam; 1:300; citrate buffer – 12 mins; manual IHC	Automated whole slide image analysis (Qupath) – Labelling Index in ROI
ANGIOGENESIS AND SMALL VESSELS	Platelet derived growth factor receptor-Beta (PDGFRb)	Marker for vascular pericytes [6]	Rabbit monoclonal Ab32570; Abcam; 1:500; ER2 – 20 mins; Leica Bondmax	Automated whole slide image analysis (Qupath) – Labelling Index in ROI Manual measurements of type 1 and 2 vessels (see text for details)
	Collagen 4 alpha 1 (COL4)	Vascular basement membrane, major structural component	Rabbit polyclonal Ab189408; Abcam; 1:100; ENZ1 – 15 mins; Leica Bondmax	Qupath/automated total vascular density and size measurements
	Smooth muscle actin (SMA)	Vascular smooth muscle cell and pericyte marker [6]	Mouse monoclonal, 1A4, Agilent DAKO; 1:500; no antigen retrieval; Ventana Discovery Ultra	Qupath/semi-automated vascular density and size measurements of type 1 and 2 vessels

1. Miners, J.S., J.C. Palmer, and S. Love, *Pathophysiology of Hypoperfusion of the Precuneus in Early Alzheimer's Disease*. *Brain Pathol*, 2016. **26**(4): p. 533-41.
2. Bankhead, P., et al., *QuPath: Open source software for digital pathology image analysis*. *Sci Rep*, 2017. **7**(1): p. 16878.
3. Gordon, B.A., *Neurofilaments in disease: what do we know?* *Curr Opin Neurobiol*, 2020. **61**: p. 105-115.
4. Yuan, A., et al., *Neurofilaments and Neurofilament Proteins in Health and Disease*. *Cold Spring Harb Perspect Biol*, 2017. **9**(4).

5. Jayakumar, A.R., A. Apeksha, and M.D. Norenberg, *Role of Matricellular Proteins in Disorders of the Central Nervous System*. *Neurochem Res*, 2017. **42**(3): p. 858-875.

6. Smyth, L.C.D., et al., *Markers for human brain pericytes and smooth muscle cells*. *J Chem Neuroanat*, 2018. **92**: p. 48-60.

Figures

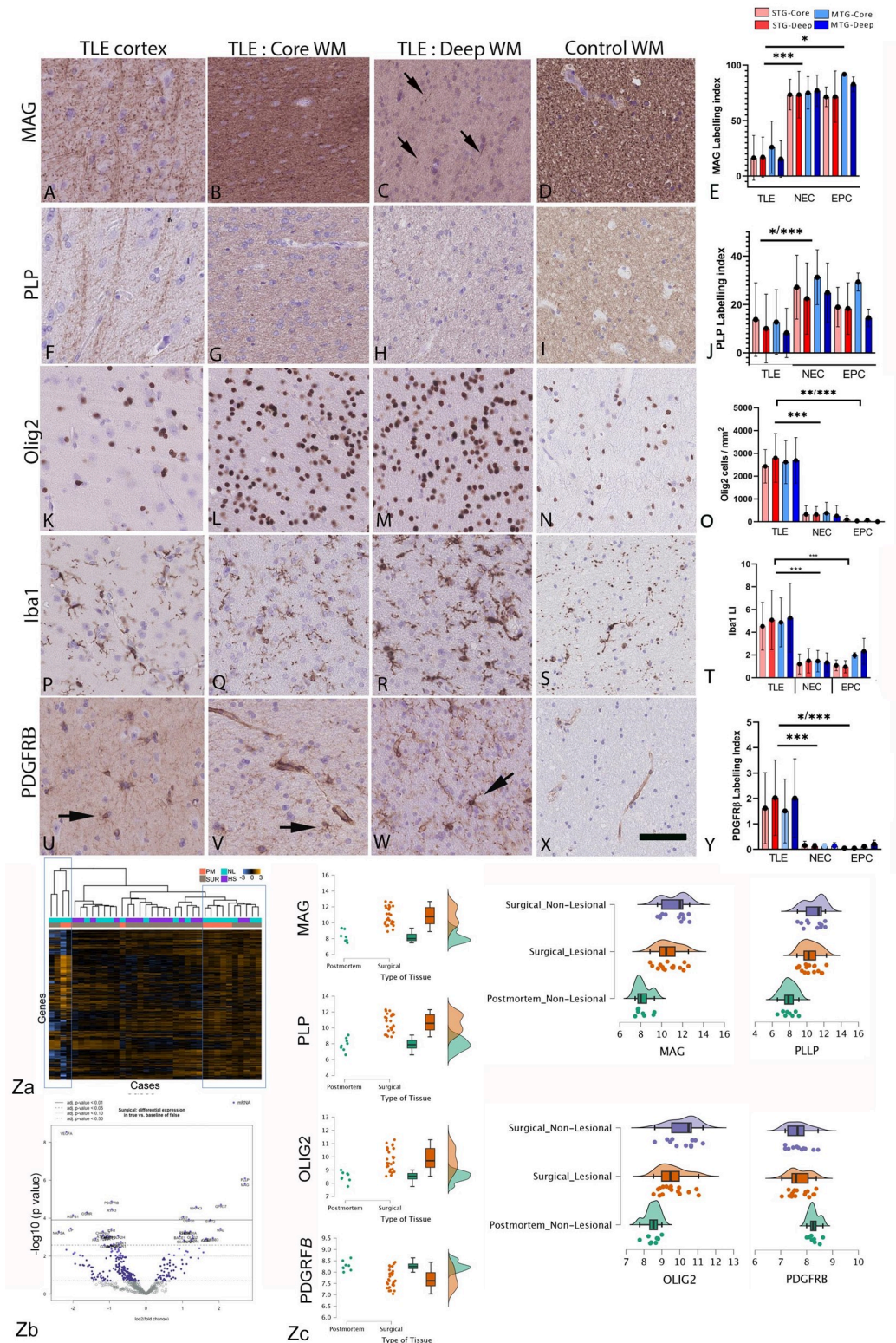


Figure 1

White matter myelin and glial marker analysis in temporal lobe epilepsy (TLE) compared to controls

Pathology quantitation (A-Y): (A). **Myelin associated glycoprotein (MAG)** in the TLE cortex labelled radial fibres and (B) diffuse, intense axonal labelling in the core white matter with (C) more patchy labeling noted in deep white matter (arrows) (D). In non-epilepsy control post-mortem (PM) cases, white matter showed more uniform and intense labelling. (E). Bar graph of quantitative analysis of MAG with significantly lower labeling index (LI) in all four regions of interest (ROI) (superior temporal gyrus (STG) core and deep and middle temporal gyrus (MTG) core and deep) in TLE compared to non-epilepsy controls (NEC) and epilepsy controls (EPC). (F). **Phospho-lipid protein-1 (PLP)** similarly labelled cortical axons and (G) core white matter with (H) weaker labelling in deep but (I) more uniform labelling noted in PM control white matter. (J). Bar graph showed significantly lower labelling in ROI in TLE compared to NEC cases. (K). **Olig2** in the cortex with diffuse white matter oligodendrogliosis in TLE cases in (L) core and (M) deep white matter, with evidence of greater densities than (N) control PM white matter (O); This was confirmed on quantitative analysis of Olig2 cell densities with significantly higher values in TLE than NEC and EPC control groups, apart from the deep white matter of the MTG in EPC. (P). **Iba1** labelling of ramified microglia in the cortex compared to (Q) core and (R) deep white matter, which both appeared greater than (S) PM control white matter qualitatively and confirmed on quantitative analysis (T) of Iba1 labelling index in all ROI which was significantly higher in TLE than controls, apart from the deep white matter of the MTG in EPC. (U) **PDGFRb** in TLE labelled scattered multipolar-glial cells in the cortex and also (V) in the core white matter (arrows) in addition to perivascular cells. (W) In the deep white matter in TLE cases there was an impression of increased overall labelling but (X) an impression of fewer PDGFRb-positive glial cells in PM controls. (Y) The labelling index for PDGFRb was higher in TLE than NEC and EPC in all ROI. Bar in X is equivalent to 50 microns approx. (redrawn scale bar from ndpi). In the bar graphs, straight lines indicate that all four ROI in the group were significantly different using non-parametric tests (Mann Whitney test). Bars with corners indicate that <4 ROI showed significance.

* $p < 0.05$, ** $p < 0.01$, *** $p < 0.001$.

Nanostring gene expression analysis of deep white matter (Za-c). (Za). Heat map of gene expression data in all groups with blue lines highlighting clustering of mainly non-lesional cases. (Zb) Volcano plot of significantly upregulated and downregulated genes in TLE surgical cases compared to PM control groups ; 135 genes showed at least one-fold significant difference between postmortem and surgical cases. (Zc) Scatter and box plots showing the distribution of the data set, including the median, interquartile ranges, minimum and maximum, for specific genes (MAG, PLLP, OLIG2 and PDGFRb) and expression in surgical lesional, non-lesional and PM control groups MAG, PLLP and Olig2 showed significantly reduced mRNA expression in postmortem cases compared with surgical cases ($p < 0.001$), whereas PDGFRb revealed higher gene expression in postmortem cases compared with surgical cases ($p < 0.001$).

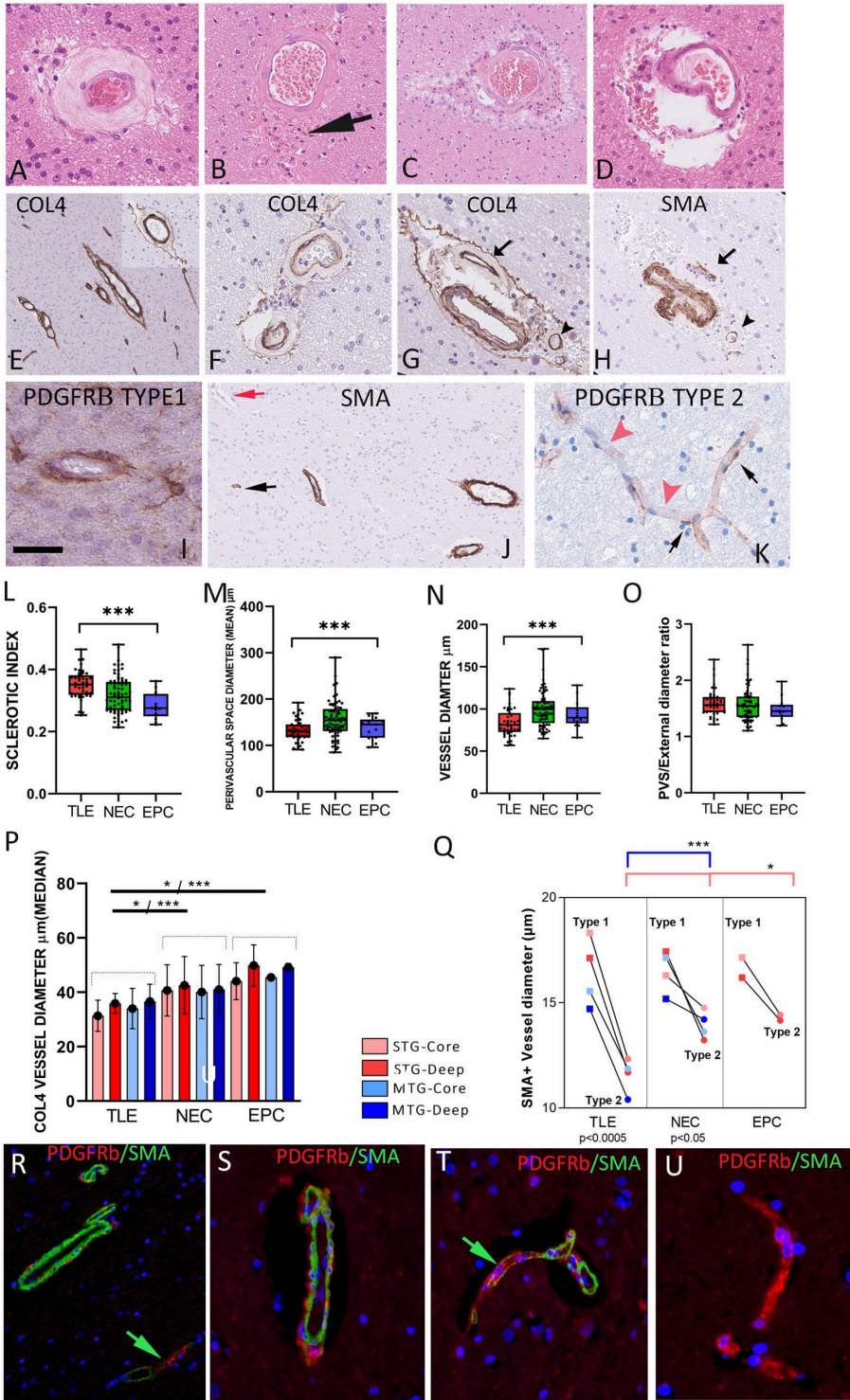


Figure 2

White matter vascular marker analysis in temporal lobe epilepsy (TLE) compared to controls.

The spectrum of white matter small vessel disease (SVD) in TLE with (A) marked arteriosclerosis with hyaline thickening of the media on H&E stain, (B) perivascular pigment laden macrophages, (C) perivascular space (PVS) dilatation and prominent corpora amylacea and (D) Perivascular space dilatation without vascular sclerosis. (E) COL4 labelling of white matter vessels of all calibre; inset showing an observation noted in some

TLE cases of splitting of the COL4 layer with intervening PVS. (F) COL4 labelling of a small vessel with sclerosis and in (G) with splitting or 'dissection' of COL4 layer. (G) and (H) show the same white matter vessels in serial sections, labelled with COL4 and SMA (arrow and arrowheads); there is sclerosis of one vessel and splitting of COL4 labelling which is not observed on SMA, although loss of SMA+ cells in the media is noted in the hyalinized vessels. (I) PDGFRb labelling of vessels with complete circumferential pericyte labelling (Type 1 vessel). (J) SMA labelling of perivascular smooth muscle cells in arterioles in addition to pericytes around small capillaries which were SMA positive (black arrow) or negative (red arrow). (K) Intermittent labelling of PDGFRb around capillary channels (Type 2 vessel). (L) Box and whisker plot (showing quartiles and maximum and minimum values) of sclerotic index in TLE cases compared to non-epilepsy control (NEC) and epilepsy control (EPC) groups. Significantly greater vascular sclerosis was noted in the TLE group. (M) Perivascular space (PVS) diameter, (N) vessel diameter and (O) the ratio of PVS to external vessel diameter are shown with lower PVS and diameter in the TLE group (Kruskal-Wallis test). (P) Bar graph of mean values of COL4 vascular diameter (microns) (and standard deviation in error bars) for all ROI in TLE, NEC and EPC groups with smaller mean values in TLE. (Q) Line graphs of SMA vascular diameters (microns) for Type 1 and Type 2 vessels in different ROIs in TLE, NEC and EPC control groups. Group differences (Mann-Whitney tests) are shown (top) and paired differences between type 1 and 2 vessel diameters within groups (Wilcoxon signed rank test, bottom), with greater significance noted in the TLE group with smaller type 2 vessels. (R-U) Double labelling (SMA/PDGFRb) of TLE cases and PM controls (S,T) confirming co-labelling of small arterioles in white matter (R,S) as well as focal co-localisation of labelling in some small capillaries (green arrows (R,T)). However, many small capillaries were devoid of SMA labelling (U). For graphs * $p < 0.05$, ** $p < 0.01$, *** $p < 0.001$. Bar is equivalent to approx.. 20 microns in A-D, 50 microns in G, H, R-U, 35 microns in I, K, 150 microns in E, J (Bar redrawn from original npdi scales).

CORE WM DEEP WM

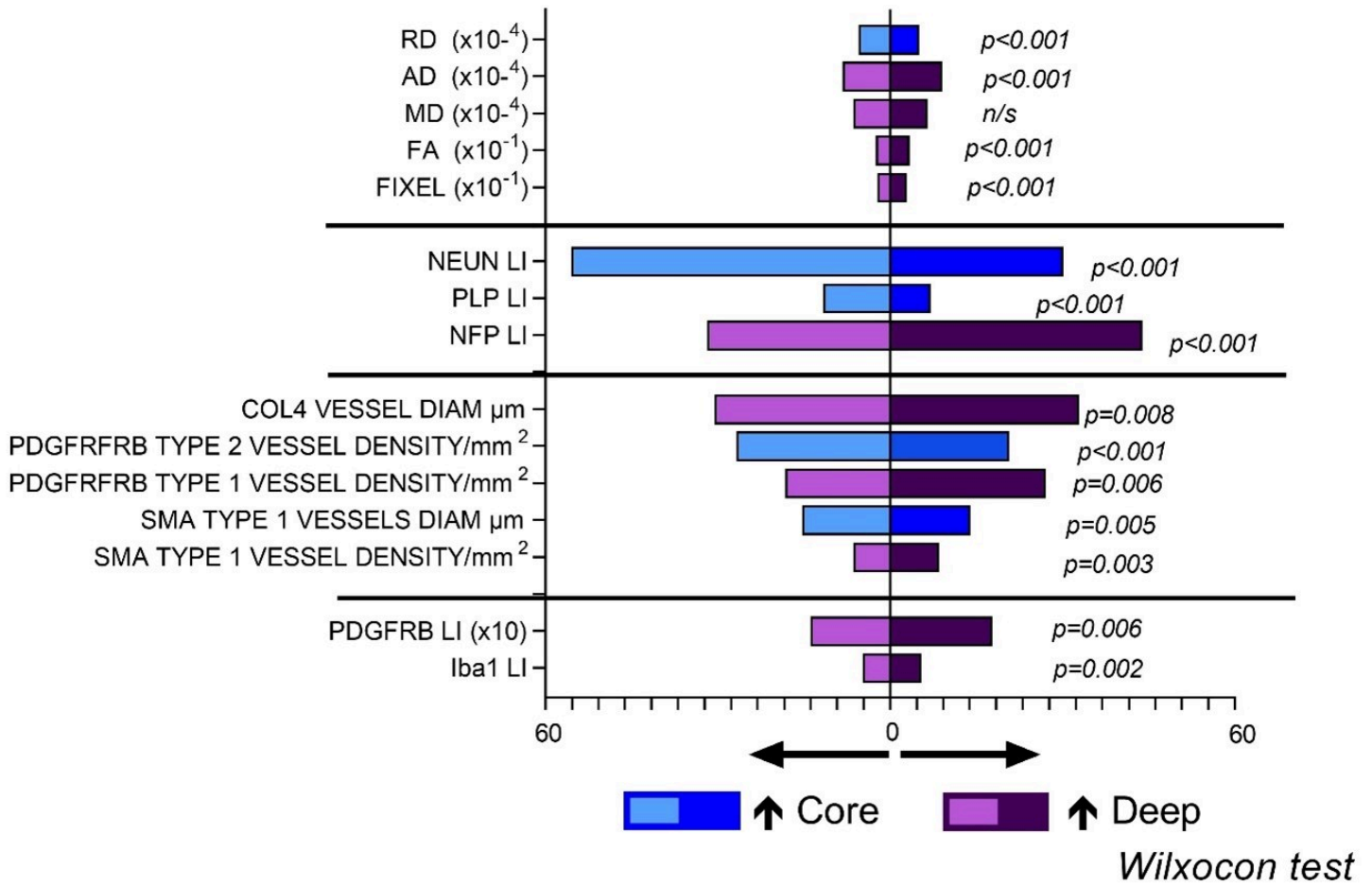


Figure 3

Comparison of deep and superficial white matter pathology and DWI variables in TLE.

Pyramid graphical representation of DWI measures (top) and pathology factors which showed significant differences between the superficial and deep white matter (data shown is average scores across all core and deep white matter regions and p values with Wilcoxon rank score test). AD = Axial Diffusivity, MD = Mean Diffusivity, RD = Radial Diffusivity, FA = Fractional Anisotropy, FIXEL = Fixel Based Analysis Measurement.

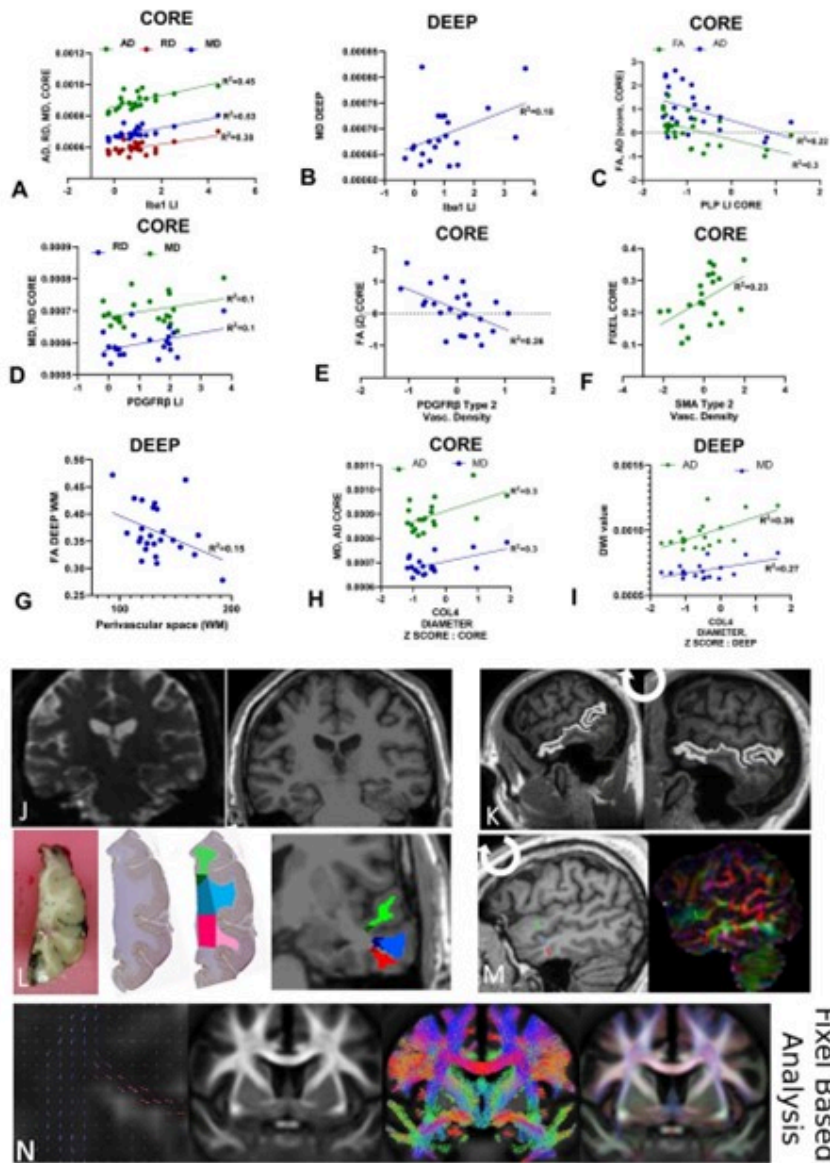


Figure 4

Diffusion weighted MRI (DWI) and Fixel based analysis (FBA) with pathology correlations.

Linear regression analysis of DWI measures averaged across either all core or deep white matter regions (also regressed using Z scores relative to control DWI data, where shown) against pathology variables in same regions (as mean scores and Z scores compared to control cases) ; date is shown where significant regressions were identified on univariate analysis (See also supplemental Table 3) : Iba labelling (A, B), Phospholipid protein (PLP) (C), PDGFRb (D, E), SMA (F), perivascular space measurement (PVS) (G) and COL4 (H, I) confirming the main associations for DWI and FBA were in the core white matter and for vascular pathology measures.

Pipeline for the DWI analysis: (J) Diffusion images following denoising, un-ringing, motion, eddy and field bias corrections were aligned to T1 and diffusions interpolated to match voxel size of T1 (1mm). (K) Middle temporal gyrus (MTG) was rotated to align flat to enable orientation with brain slice, (L) Regions of interest (ROI) in white matter (superior temporal gyrus green shades, middle temporal gyrus blue shades, inferior

temporal gyrus red shades with deeper colour shade representing deep ROI) were best matched and co-registered on MRI and pathology histological sections using Freesurfer white matter parcellation to manually segment gyri into the core and deep white matter (note the histology sections shown for illustration only or MRI and not aligned to MRI slice). (M) MRI images were then rotated back to extract diffusion tensors for each region. (N) Fixed-based-analysis (Left to right) : 1. Individual orientation distribution function (ODF) were calculated, 2. registered to create a healthy population template, 3. which was used to create a SIFT filtered tractogram, for 4. Fixel-based analysis. RD = Radial Diffusivity, AD = Axial Diffusivity, MD = Mean Diffusivity, FA = Fractional Anisotropy, FIXEL = Fixel Based Analysis Measurement, LI = labelling index.

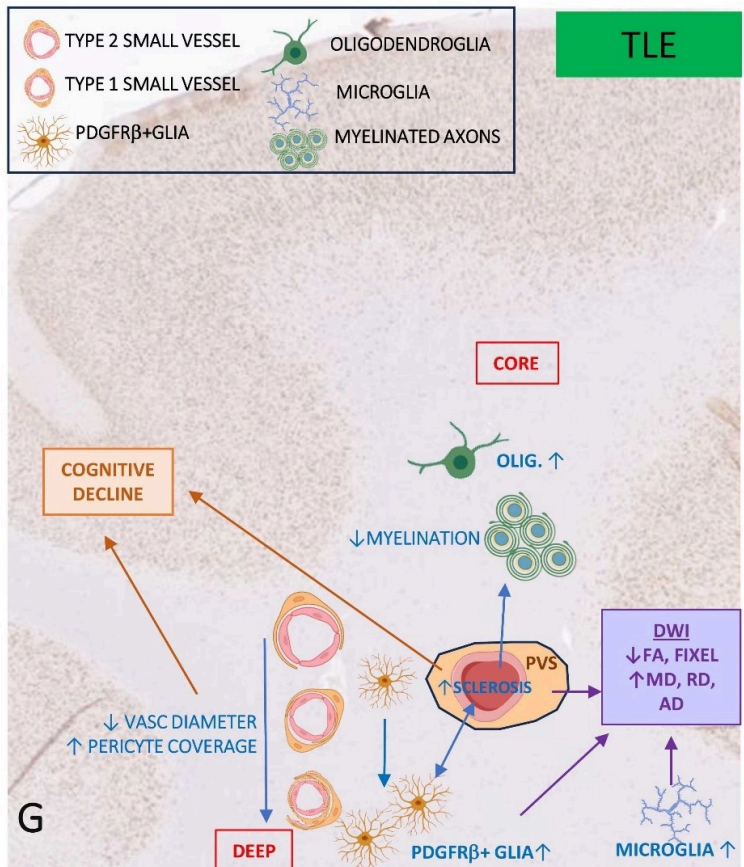
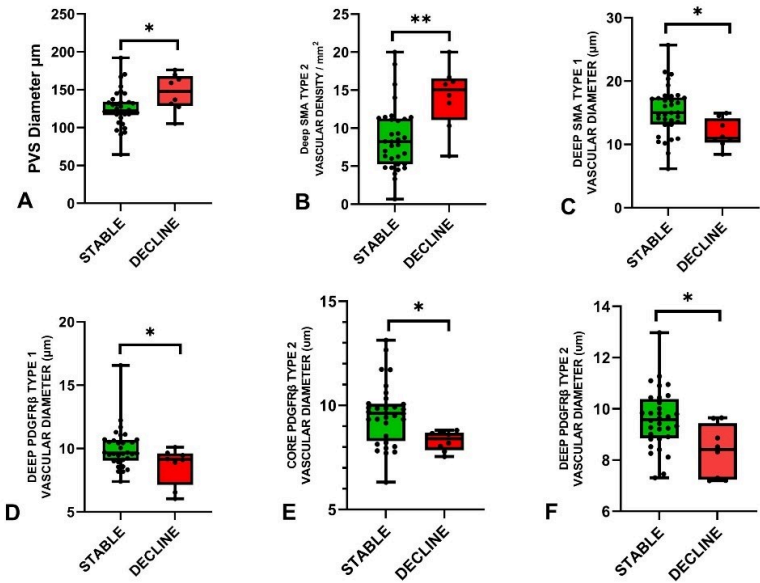


Figure 5

Correlations with microvascular pathology and neuropsychology.

(A-F). Logistic regression analysis of pathology measures in groups with and without pre-operative verbal cognitive impairment (see also Supplemental table 4) showing significant differences in vascular pathology measures in the decline group, represented graphically as box plots (median, 25th and 75th centile, range) : (A) Perivascular space (PVS) and (B) SMA type 2 vascular density were increased in the decline group whereas (C) SMA type 1 vessel diameter (D) PDGFRb vessel diameter, (E) PDGFRb type 2 vessel diameter in core and (F) deep white matter were significantly reduced. (G). Summary diagram based on all observations of regional alterations and relationship of small vessels measurements with other cellular components in TLE white matter (blue text and arrows) and which factors might impact on DWI changes (purple arrows) and cognition (brown). In brief, temporal lobe epilepsy is associated with both increased arteriolosclerosis and vascular pericytes; the later may represent a protective adaptation. Increased parenchymal PDGFRb cells, which correlate with degenerative vascular sclerosis, are increased particularly in the deep white matter. Epilepsy is associated with white matter oligodendrogliosis and microglial increase, the latter particularly in deep regions. Increased perivascular space and reduced small vessel size are linked to cognitive decline. DWI alterations in the core are mainly influenced by increased glia density, PVS and small vessel changes. Icons created with *Biorender*.

Supplementary Files

This is a list of supplementary files associated with this preprint. Click to download.

- [SupplementalTable1.pdf](#)
- [SupplementalTable2.docx](#)
- [SupplementalTable3.docx](#)
- [SupplementalTable4.docx](#)
- [SupplementalFigures.docx](#)
- [Supplementalmethods.docx](#)